Time-dependent photoconductivity in the presence of light-induced recombination: application to atactic polystyrene

1989 J. Phys.: Condens. Matter 1 4367

(http://iopscience.iop.org/0953-8984/1/27/009)

J. Phys.: Condens. Matter **1** (1989) 4367–4380. Printed in the UK

Time-dependent photoconductivity in the presence of light-induced recombination: application to atactic polystyrene

C Tannous†‡, G Leclerc† and A Yelon†

† Groupe des Couches Minces and Department of Engineering Physics, Ecole Polytechnique, Box 6079, Station 'A', Montréal, Québec, Canada H3C 3A7

‡ Physics Department, The University of Western Ontario, London, Ontario, Canada N6A 3K7

Received 1 June 1988, in final form 31 October 1988

Abstract. After introducing a novel recombination term representing light-induced bimolecular recombination processes we calculate time-dependent profiles for electron and hole density and electric field across a highly insulating material (atactic polystyrene) subjected to ultraviolet radiation and to the application of a potential at the illuminated electrode. The time-dependent current density is calculated for a wide range of parameters over arbitrary long intervals of time. In the weak-field limit the asymptotic behaviour of the photocurrent follows the Onsager electron–hole pair generation mechanism as observed experimentally in the strong-field case.

1. Introduction

The electrical behaviour of highly insulating polymers is, in general, quite complicated experimentally, and difficult to model. The dark conductivity of 'virgin' atactic polystyrene, which has been cast in the dark and never exposed to light, is very different from that measured after exposure to light [1]. This may be due to a space charge, which may be formed by photo-emission or by separation of the heavy electrons and light holes and deep trapping of holes. In our case the space charge is believed to be trapped electrons; it is generated by the illumination, and is extremely stable thereafter. Passage of current, presumably due to holes (although ionic conductivity may also play a role in this material [2]), does not affect this space charge. The photoconductivity of this material, which can be observed only on non-virgin samples (time constants are too long to permit measurements of virgin material) is also very complicated [3].

While less severe problems arise in 'good' photoconductors, Chance and Braun have reported [4] differences in behaviour between virgin and non-virgin samples of anthracene, and they modelled only the behaviour of the simpler, virgin material. Such effects may be compared with, and are perhaps related to, the Staebler–Wronski effect in amorphous silicon [5] and to the photo-effect in chalcogenide glasses [6]. The nature of photo-effects in insulating polymers is far less clear. However, there are a certain number of conditions that any model must satisfy.

0953-8984/89/274367 + 14 $02.50

If the creation of electron–hole pairs by light produces trapped electrons which do not recombine in the dark, even in the presence of an injection current, then illumination must also lead to recombination. Otherwise, the space charge would increase indefinitely, which is not the case. The mechanism for such a light-induced effect could be simply the production of transitory recombination centres, or it could be a directly stimulated process. In either case, existing models of photoconductivity [4, 7] or of electron-beam-induced conductivity [8–10] do not allow for such a mechanism.

We present here a model that conforms as closely as possible to what we believe is an appropriate description of conductivity and photoconductivity in atactic polystyrene [1, 3]. This includes the possibility of hole injection currents, a fixed value for the hole mobility (any trapping is assumed merely to contribute to this value) and negligible mobility for electrons, pair generation by the Onsager mechanism, and the light-induced recombination, which is the main new feature. The UV light, which is capable of generating pairs, has a penetration length that is short compared with the sample length.

As we wish to take account of the exponential decay of the light intensity, and of the true field and charge profiles which result, it is not possible to establish a true steady-state solution. If we wait extremely long times, pairs will be present at any distance from the origin. The calculation is therefore a dynamic one, with an effective steady state established at times long compared with the drift times of the carriers. This approach is formally similar to the one adopted by Donovan and Wilson [11] in the case of PDATS (the polymer bis(*p*-toluene sulphonate) ester of 2,4-hexadiyne-1,6-diol) and has the advantage, however, that we obtain information concerning the evolution of the system with time.

We base our approach on the semiconductor equations, which are essentially the continuity equations for electrons and holes and Poisson's equation. These are expected to be valid for the low-field regime we are interested in. Since we perform a time-dependent simulation under variable illumination and applied voltage, the semiconductor equations are subjected to time-dependent boundary conditions. We transform the equations in a way such that the time-dependent boundary-condition problem is mapped onto an initial-value problem. The values obtained for the electric field profile in the sample, the electron and hole density profiles are checked with Poisson's equation at each point and each timestep. Moreover, the overall solution is tested by recalculating the voltage difference and comparing it to the applied one at each timestep.

The asymptotic values of the photocurrent are found to obey the Onsager electron–hole pair generation mechanism at low fields in agreement with the experimental behaviour at high fields and with the expected analytic long-time limit of the model considered.

This paper is organised as follows. Section 2 contains the model and the equations of motion we use. Section 3 presents the solution of the equations. Section 4 contains a description of the simulation results. Section 5 is devoted to the discussion and conclusions.

2. Model

Consider a parallel-plate capacitor geometry with a photoconducting semiconductor or polymer as the dielectric. Assuming that the distance between the capacitor plates is much less than the lateral dimensions of the plates with light uniformly illuminating one of the plates, the problem is essentially one-dimensional. The dynamics of the carriers

is given by the continuity equations for the electrons and holes and by the Poisson equation.

Since the electrons are assumed immobile, the time dependence of their concentration is given by

$$\partial n/\partial t = G(x) - R(x)np. \tag{1}$$

We assume a bimolecular recombination mechanism, represented by R, and the same generation mechanism, represented by G, for both types of carriers.

The continuity equation for the holes is

$$\frac{\partial p}{\partial t} = \frac{\partial}{\partial x}\left(D_p \frac{\partial p}{\partial x} + \mu_p p \frac{\partial \psi}{\partial x}\right) + G(x) - R(x)np. \tag{2}$$

Here, μ_p and D_p are field-independent mobility and diffusion coefficient for holes. In contrast to most treatments [12], we do not neglect the diffusion term. In the presence of the static electron space charge, its importance is not obvious. In addition, its inclusion does not significantly complicate the mathematical treatment to be used in the solution of the problem.

The potential, $\psi(x, t)$, satisfies the Poisson equation

$$\partial^2 \psi/\partial x^2 = (e/\varepsilon)[n(x, t) - p(x, t)] \tag{3}$$

where e denotes the electric charge and ε is the dielectric constant of the material.

The application of a constant voltage requires that the electric field $E(x, t)$ satisfy

$$\int_0^L [\partial E(x, t)/\partial t]\, \mathrm{d}x = 0 \tag{4}$$

where L is the thickness of the sample. Using equation (4), the definition, $E = -\partial \psi/\partial x$, and the expression for the total current

$$J(x, t) = ep\mu_p E - eD_p(\partial p/\partial x) + \varepsilon(\partial E/\partial t) \tag{5}$$

we may write an evolution equation for the electric field:

$$\frac{\partial E}{\partial t} = \frac{e\mu_p}{\varepsilon L}\int_0^L pE\, \mathrm{d}x - \frac{eD_p}{\varepsilon L}[p(L, t) - p(0, t)] - \frac{e\mu_p}{\varepsilon} pE + \frac{eD_p}{\varepsilon}\frac{\partial p}{\partial x}. \tag{6}$$

Equations (1), (2) and (6) constitute the system of coupled time-dependent partial differential equations that we wish to solve. Before we proceed to solve the equations, we need explicit forms for G and R.

We neglect thermal generation and assume that

$$G(x, t) = \eta I. \tag{7}$$

Here, η is the photogeneration efficiency, and I is the absorbed intensity per unit thickness, given by

$$I = F\alpha \exp(-\alpha x)/[1 - \exp(-\alpha L)] \tag{8}$$

where F is the incident flux of UV radiation, and α is the absorption coefficient.

In accordance with experimental evidence for polystyrene [3], we take η from the Onsager theory of field-dependent geminate recombination. To first order in the electric field, the quantum efficiency is given by

$$\eta(r_0, E) = \eta_0 \exp\left(-\frac{r_c}{r_0}\right)\left(1 + \frac{er_c}{2k_B T}E(x,t)\right). \tag{9}$$

In equation (9), η_0, the primary quantum yield, is the number of thermalised ion pairs per absorbed photon, r_0 is the thermalisation length, and r_c is the critical distance separating geminate charges beyond which instantaneous recombination may be avoided. Considering the hole as a sink sitting at the origin, one may estimate the latter distance by equating the thermal energy $k_B T$ to the Coulomb energy of the electron in the field of the hole when their mutual separation is r_c. Therefore

$$r_c = e^2/4\pi\varepsilon k_B T \tag{10}$$

where k_B is Boltzmann's constant and T is the temperature.

As discussed above, we assume that light induces bimolecular recombination:

$$R = \frac{\sigma F}{n_0}\frac{\exp(-\alpha x)}{(1 - e^{-\alpha L})} \tag{11}$$

where σ is an effective cross section and n_0 is an effective carrier density. The ratio σ/n_0 is our sole parameter that we vary in order to obtain agreement with the experimental values. All the other parameters used are taken from the experiment.

Finally, the initial condition for the calculation is the presence of a steady-state hole injection current, produced by the voltage V applied at the illuminated electrode, in the absence of any electron space charge ('virgin' material). The calculation of this current, for arbitrary field at the injecting electrode is described in the Appendix (see also [13]). The use of this condition, rather than assuming that the field and light are applied at the same time, facilitates and accelerates convergence of the solution.

3. Solution of the equations

One possible way to integrate the system of equations (1), (2) and (6) is to make repetitive use of the Taylor expansion

$$Z(x, t + \Delta t) = Z(x, t) + (\partial Z/\partial t)\Delta t \tag{12}$$

where Z stands for n, p or E, and Δt is the timestep. Instead, we use the method of lines [14] for space discretisation of equation (12), turning the system of equations into one of first-order coupled ordinary differential equations, which may be numerically integrated by Runge–Kutta methods, or any other algorithm appropriate for solving initial-value problems [15]. Transforming a boundary-value problem into an initial-value one with the help of (4) is similar somehow to the method of invariant embedding which is of considerable use in physical problems [16].

The numerical scheme, being explicit, embodies one major problem of stability. This is related to the choice of the integration timestep, Δt. Two tests are used to determine this step, the first local and the second global. By repetitive use of (12), the values $n(x, t)$,

$p(x, t)$ and $E(x, t)$ are determined at any time t and any point x. By monitoring at the grid points and at each time the quantity

$$\Delta(x, t) = |(e/\varepsilon)[n(x, t) - p(x, t)] + (\partial E/\partial x)| \tag{13}$$

we may check the values of the carrier concentrations and of the electric field. The global test consists of monitoring the quantity

$$\delta(t) = \left| \int_0^L E(x, t)\, \mathrm{d}x - V \right| \tag{14}$$

at each timestep. In equation (14), V is the voltage drop between the illuminated front plate and the back plate.

Decreasing the value of the timestep Δt results in a decrease of the values of $\Delta(x, t)$ and $\delta(t)$ as expected from numerically explicit schemes of integration. However the smaller the value of Δt, the longer we have to run the system in order to observe significant variations in the behaviour of the physical quantities $n(x, t)$, $p(x, t)$, $E(x, t)$ and the total time-dependent photocurrent

$$J(t) = \frac{e\mu_p}{L} \int_0^L pE\, \mathrm{d}x - \frac{eD_p}{L}[p(L, t) - p(0, t)]. \tag{15}$$

Hence, a trade-off value of Δt is necessary, such that it keeps the error small and allows the observation of significant variations in the physical quantities of interest.

We find that the appropriate value of Δt is a fraction of the characteristic time, τ_0, of the system, given by

$$\frac{1}{\tau_0} = \frac{\mu_p V}{L^2} + \frac{\sigma F \varepsilon V}{n_0 e L^2} \tag{16}$$

indicating that τ_0 is the harmonic mean of a typical drift time $\mu_p V/L^2$ across the sample and the time constant for light-induced recombination processes. Depending on the values of the physical parameters, τ_0 may range from hours to a small fraction of a second. This is discussed in the next section.

4. Results

In what follows, we have held certain parameters constant, and varied others. We have taken [3] $\mu_p = 1.0 \times 10^{-16}\ \mathrm{m^2\ V^{-1}\ s^{-1}}$. From the Einstein relation [17] this implies $D_p = k_B T \mu_p / e = 2.54 \times 10^{-18}\ \mathrm{m^2\ s^{-1}}$ at $T = 295$ K. The relative dielectric constant is [18] $\varepsilon_r = 2.55$.

The parameters for the Onsager mechanism are [3] $\eta_0 = 0.5$ and $r_0 = 1.6 \times 10^{-10}$ m. The absorption constant α is [18] $10^7\ \mathrm{m^{-1}}$. As both n_0 and σ are unknown, we take $n_0 = 10^{22}\ \mathrm{m^{-3}}$ and allow σ to vary. We also vary V and F, which are experimental parameters. In the calculations in which we do this, we take the field at the injecting electrode as $9.5 \times 10^4\ \mathrm{V\ m^{-1}}$ when the applied voltage $V = 8.0$ V and $5.0 \times 10^4\ \mathrm{V\ m^{-1}}$ when $V =$

Table 1. Values of the current in the dark ($t = 0$) and in the presence of illumination at saturation ($t \rightarrow \infty$) for different values of V and σ. These results are obtained for a given value of F at 8.0×10^{18} photons s^{-1} m^{-2}. The value of the electric field at the injecting electrode for the following values of the applied voltage $V = -8.0$, 8.0, -3.0 and 3.0 V is -7.94×10^5, 9.5×10^4, -2.95×10^5 and 5.0×10^4 V m^{-1} respectively. These values ensured the same absolute value of the dark current for both signs of a given applied voltage.

Voltage (V)	Cross section, σ (10^{-4} cm^{-2})	Dark current, $J(t = 0)$ (10^{-14} A cm^{-2})	Photocurrent at saturation, $J(\infty)$ (10^{-14} A cm^{-2})
−8.0	10^{-17}	−0.473	−0.695
	10^{-18}	−0.473	−1.175
	10^{-19}	−0.473	−2.720
	10^{-20}	−0.473	<−3.2
8.0	10^{-17}	0.473	0.520
	10^{-18}	0.473	0.615
	10^{-19}	0.473	0.745
	10^{-20}	0.473	0.950
−3.0	10^{-17}	−0.0651	−0.155
	10^{-18}	−0.0651	−0.345
	10^{-19}	−0.0651	−0.940
	10^{-20}	−0.0651	<−2.4
3.0	10^{-17}	0.0651	0.110
	10^{-18}	0.0651	0.122
	10^{-19}	0.0651	0.186
	10^{-20}	0.0651	0.475

Table 2. Values of the current in the dark ($t = 0$) and in the presence of illumination at saturation ($t \rightarrow \infty$) for different values of the electric field at the injecting electrode. The results are obtained when the values of the voltage applied V, cross section σ and incident flux F equal 8.0 V, 10^{-19} m^{-2} and 8.0×10^{18} photons s^{-1} m^{-2} respectively.

Electric field (V m^{-1})	Dark current density, $J(0)$ (10^{-14} A cm^{-2})	Photocurrent density at saturation (10^{-14} A cm^{-2})
9.4×10^4	0.474	0.75
2.0×10^5	0.406	0.80
5.3×10^5	0.005	0.90

3.0 V (see table 1). However we have also varied this field, while holding V, F and σ constant (see table 2). In figure 1, we show the spatial variation of a typical profile of hole density at various times. The profile is relatively flat at $t = 0$, in the dark.

After the light is switched on, the value of the hole density increases rapidly at the illuminated electrode. The profile then becomes smoother as the holes readjust.

The electron profile, which is zero at any point x for $t = 0$, jumps to a value comparable with that of the hole density. However, its spatial variation does not change much with time. The concentration drops rapidly with depth, as might be expected (figure 2).

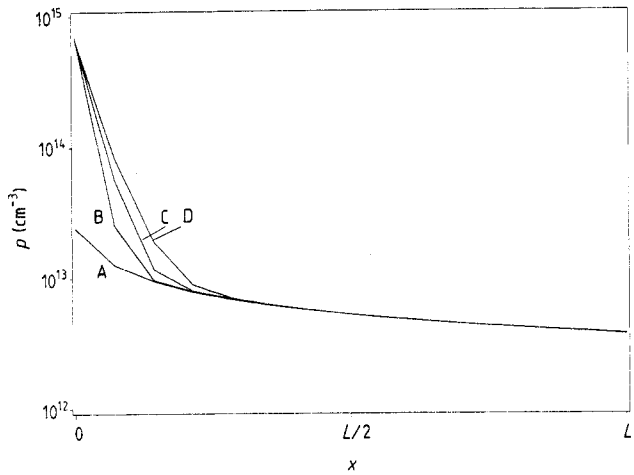

Figure 1. Hole density profile at various times. Curve A corresponds to the profile in the dark whereas B, C and D correspond to a time equal to 100, 400 and 1000 timesteps respectively. The timestep is 14.06 s. The applied voltage $V = 8.0$ V, $\sigma = 10^{-19}$ m^{-2}, the incident flux $F = 8.0 \times 10^{18}$ photons s^{-1} m^{-2} and the electric field at the injecting electrode is 9.5×10^{4} V m^{-1}.

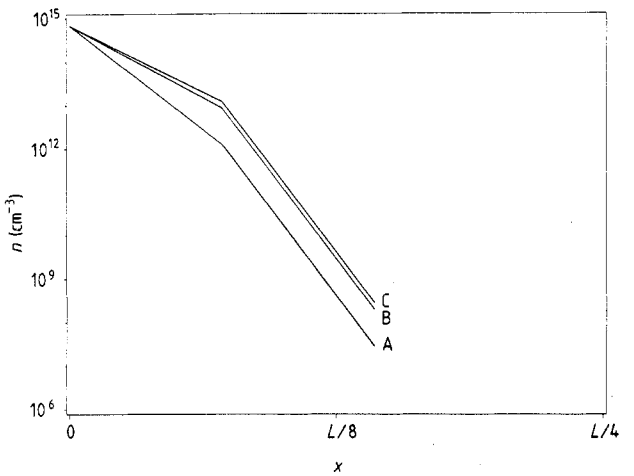

Figure 2. Electron density profile at various times. In the dark the electron profile is zero for all values of x. Curves A, B and C correspond to a time equal to 100, 400 and 1000 timesteps respectively. The value of the timestep and the rest of the parameters are the same as in figure 1. Beyond $x \simeq L/8$, $n(x)$ is essentially zero.

The form of $E(x, t)$ is different depending upon the sign of V. For $V < 0$, $E(x, t)$ evolves such that at any time it is a convex function of x (figure 3), whereas the opposite is observed for $V > 0$ (figure 4).

Turning to the results for the photocurrent versus time it is observed that, when the applied voltage is negative, the absolute value of the current increases smoothly with time, reaching a saturation regime faster for higher incident radiation flux F. For the highest value of F considered (10^{20} photons s^{-1} m^{-2}) the saturation is reached almost

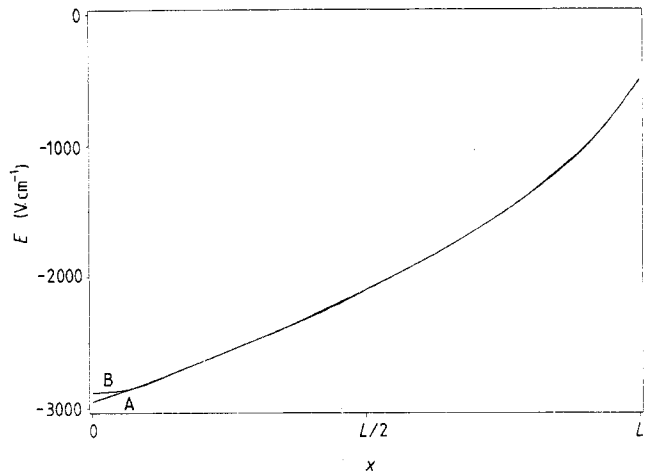

Figure 3. Electric field profile for a negative applied voltage for two instants of time. Curve A corresponds to the profile in the dark whereas B corresponds to 1000 timesteps. Here, the timestep is 0.075 s. The applied voltage is -3.0 V, the cross section $\sigma = 10^{-19}$ m^{-2}, the incident flux is 8.0×10^{18} photons s^{-1} m^{-2} whereas the electric field at the injecting electrode is -2.95×10^{5} V m^{-1}.

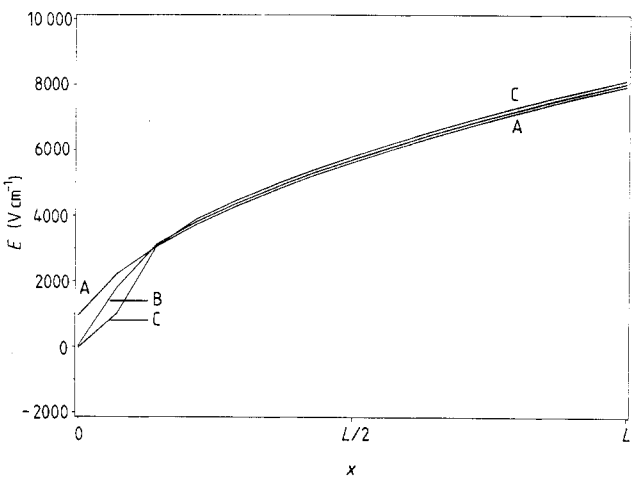

Figure 4. Electric field profile at various times for a positive applied voltage. Curve A corresponds to the profile in the dark whereas B and C correspond to 400 and 1000 timesteps respectively. The timestep and all the other parameters are the same as in figure 1.

instantaneously. In addition, the absolute value of the current at saturation increases [19] with F (figure 5).

When the applied voltage V is positive the magnitude of σ affects the way the photocurrent behaves as a function of time. For relatively small values of σ the photocurrent increases, reaches a maximum at a given time and then starts falling until saturation is reached (figure 6). The maximum is sharper for larger values of the flux F and is visible at earlier times, whereas the saturation value is pushed progressively to later times and to slightly higher values (figure 7).

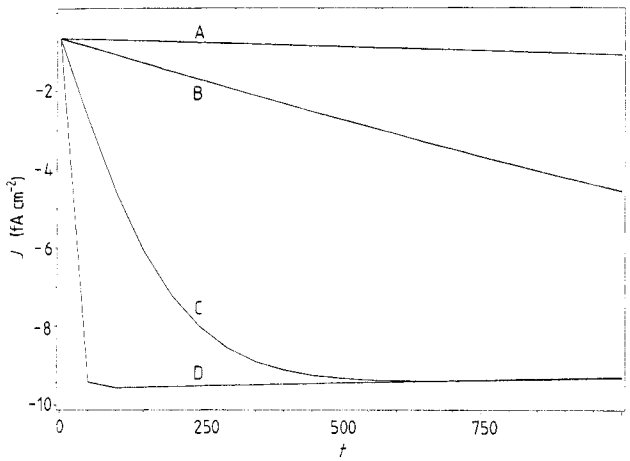

Figure 5. Current density as a function of time for various values of the incident flux F at negative applied voltage. Curves A, B, C and D correspond to F equal to 0.1, 1.0, 10.0 and 100.0 units of 10^{18} photons s^{-1} m^{-2} respectively. All curves start from the same point $J(t = 0) = -0.651 \times 10^{-15}$ A cm^{-2}, the dark current density value. The time is measured in units of a timestep equal to 0.075 s. The latter and the remaining parameters are the same as in figure 3.

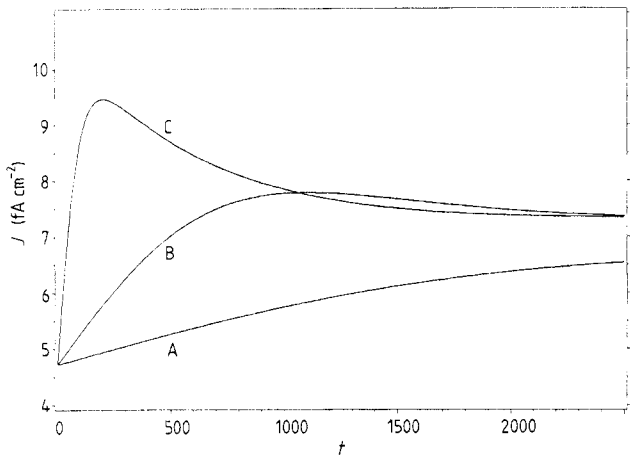

Figure 6. Current density as a function of time for low and intermediate values of the incident flux F at positive applied voltage and small σ. Curves A, B and C correspond to F equal to 0.01, 0.05 and 0.5 units of 10^{18} photons s^{-1} m^{-2} respectively. All curves start from the same dark current density value of 0.473×10^{-14} A cm^{-2}. The time is measured in units of a timestep equal to 2.81 s. The latter and the rest of the parameters are the same as in figure 1.

This behaviour indicates that light-induced recombination processes are not sufficient at short times to limit the increase in current due to the relatively small number of recombination events.

On the other hand, when σ is relatively large (figure 8) recombination forces the current to saturate gently, at short times and small values of flux F, without going through a maximum. Increasing F makes the saturation time shorter, the initial rise in the current steeper and the saturation value of the current larger.

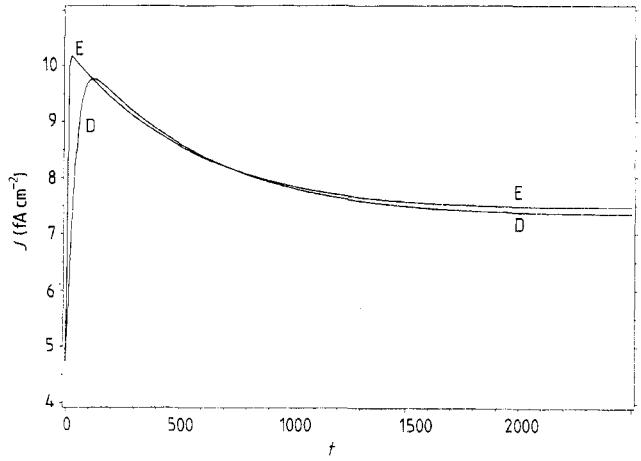

Figure 7. Current density as a function of time for large values of the incident flux F at positive applied voltage and small σ. Curves D and E correspond to F equal to 1.0 and 10.0 units of 10^{18} photons s^{-1} m^{-2} respectively. All other parameters are the same as in figure 6.

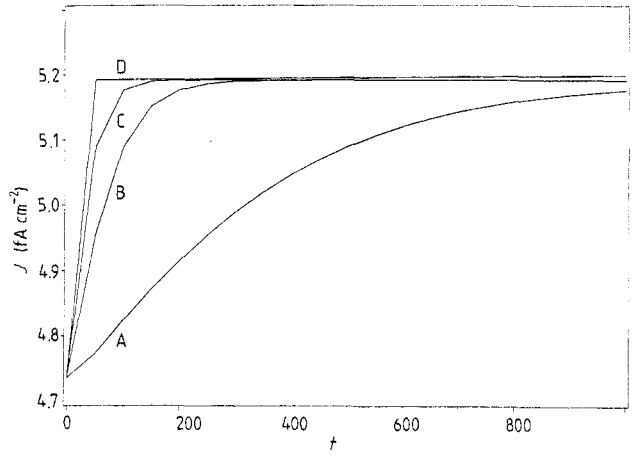

Figure 8. Current density as a function of time for various values of the incident flux F at positive applied voltage and large σ. Curves A, B, C and D correspond to F equal to 0.1, 0.5, 1.0 and 10.0 units of 10^{18} photons s^{-1} m^{-2} respectively. All curves start from the same current density value of 0.473×10^{-14} A cm^{-2}. The time is measured in units of a timestep equal to 0.281 s. The applied voltage $V = 8.0$ V, the cross section $\sigma = 10^{-17}$ m^{-2} whereas the electric field at the injecting electrode is taken as 9.5×10^4 V m^{-1}.

Keeping the magnitude of the flux F fixed, table 1 shows that, for the same value of σ and absolute value of V, the absolute value of the saturation current is larger for $V < 0$ than for $V > 0$. In this table we show some results for the saturation value of the photocurrent in comparison with the dark value for given values of the applied voltage and the recombination cross section σ.

In table 2 we show how the initial electric field at the illuminated plate affects the value of the dark current after having illuminated the material and the saturation photocurrent for given values of the applied potential and recombination cross section.

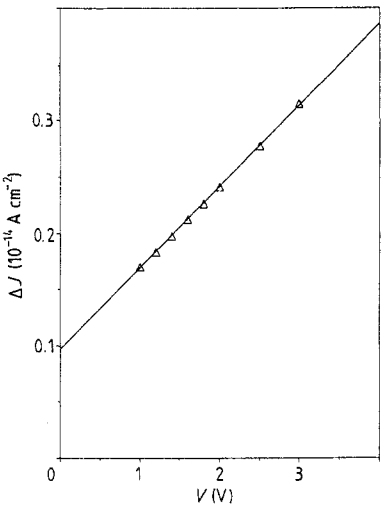

Figure 9. Difference ΔJ between the asymptotic value of the photocurrent and the dark current value versus voltage applied at the illuminated electrode. The initial electric field at the positive electrode is held fixed at the value of 0.5×10^5 V m^{-1} for all applied voltages. The rest of the parameters used are the same as those of figure 1. The typical Onsager linear dependence with a non-zero intercept of the yield versus the applied field is observed.

Although the dark current is strongly affected by the initial electric field, the asymptotic value of the photocurrent after the illumination is only slightly affected. This is important from the experimental point of view (since the electric field is not accessible to any easy measurement) as well as from the numerical simulation one (it indicates that the problem at hand is not ill-conditioned).

The ultimate overall check of our results is the dependence of the saturation photocurrent upon the applied voltage. In figure 9, the difference between the values of the photocurrent at saturation and in the dark is shown versus the applied voltage. From the Onsager theory of geminate recombination, the photo-yield, being proportional to this difference, is expected to vary linearly with respect to the applied field when the latter is weak. This is exactly what we observe in agreement with the experimental behaviour probed at higher fields in which case the photo-yield varies somehow more rapidly before it saturates to unity [3].

5. Discussion and conclusions

We have studied time-dependent effects on carrier densities, electric field and photocurrent in the presence of a novel light-induced recombination process. This process is bimolecular with an amplitude directly proportional to the local light intensity. Using the method of lines, the set of partial differential equations is transformed into a set of ordinary differential equations and the problem is transformed from a two-point boundary-value to an initial-condition one. The solution of the differential system at any arbitrary time is obtained by an extremely fast and efficient method based on an explicit scheme enabling us to explore the long-time regime of the system for a wide interval of selected parameters.

During the calculation we have used various local and global checks in order to make sure that the results we obtain are free of numerical artefacts. For a given choice of voltage drop across the sample we may choose a value of the field at the contact or alternatively the number of carriers at the contact such that the Poisson equation and the continuity equations are obeyed everywhere in the sample.

The monitoring of various conserved quantities during the time of simulation resembles molecular-dynamics simulations of fluid mechanics or statistical physics, where energy, volume or temperature of the system are constants of motion. In our case, the voltage across the sample is one global constant of motion whereas neutrality is another local constant of motion.

Within the domain of parameters that we have explored, we have obtained the detailed time variation of carrier density profiles, electric field profile and current density as a function of applied voltage, light flux and various initial conditions.

After choosing the latter such that the initial current density changes sign with the applied voltage we observed that the long-time limit of the photocurrent is not the same for fields applied at the front and the back electrodes. However the asymmetry appears, within the range of parameters we have been able to explore, to be opposite to that observed experimentally for polystyrene [3] in the strong-field case. On the other hand, from the long-time behaviour of the photocurrent, we obtained the yield to follow the Onsager model for weak fields in agreement with the experimental behaviour at strong fields. However, the long-time values of the photocurrent density are independent of the light flux whereas in the experiment (figure 6 of [3]) they behave in a linear fashion with respect to the light flux. It is not clear whether this is due to strong-field effects that our theory has not accounted for, or to metastability. From an experimental viewpoint, it is hard to know how long one has to wait in order to rule out metastability effects.

Finally, it is extremely difficult to undertake a measurement of the photo-yield for weak applied fields [3], and therefore a theory for photoconduction in atactic polystyrene valid especially in the strong-field case is needed. This effort, aiming to establish such a theory along the same lines of thought described in this work, is in progress.

Acknowledgments

This work is supported partially by the NSERC of Canada and Fonds FCAR of Quebec. CT acknowledges support from 'Programme expérimental de soutien à l'emploi scientifique'. CT wishes to thank Professor P-G de Gennes for an illuminating discussion concerning this work.

Appendix. Determination of initial conditions

The sample is in the dark for times $t < 0$. We consider the system in stationary state with no electrons excited. The dark photocurrent is entirely due to the holes, which are moving under the action of the potential drop V between the two faces of the sample.

In the stationary state and absence of electrons the systems (1), (2) and (3) reduce to

$$\mathrm{d}p/\mathrm{d}x = \mu_p pE/D_p + C/D_p \tag{A1}$$

$$\mathrm{d}E/\mathrm{d}x = (e/\varepsilon)p \tag{A2}$$

where $C = -J/3$, J being the dark photocurrent given by (15) for $t < 0$. In addition we have the constraint on the field:

$$V = \int_0^L E(x)\,\mathrm{d}x. \tag{A3}$$

The general exact solution of the system (A1), (A2) is given by

$$E(x) = \frac{\lambda^{1/3} eC}{D_p \varepsilon}\left(\frac{C_2(\mathrm{Ai})_y + C_3(\mathrm{Bi})_y}{C_2\mathrm{Ai}(y) + C_3\mathrm{Bi}(y)}\right) \tag{A4}$$

where C_2, C_3 are constants of integration,

$$y = -\lambda^{1/3}\left[\frac{\mu_p x e C_2}{2D_p^2 \varepsilon} - \frac{\mu_p C_1}{2D_p}\right]$$

$\mathrm{Ai}(y)$ and $\mathrm{Bi}(y)$ are Airy integrals, whereas

$$(\mathrm{Ai})_y = \frac{\mathrm{d}\,\mathrm{Ai}(y)}{\mathrm{d}y} \qquad \text{and} \qquad (\mathrm{Bi})_y = \frac{\mathrm{d}\,\mathrm{Bi}(y)}{\mathrm{d}y}$$

denote their corresponding derivatives. The two constants λ and C_1 are given by

$$\lambda = \left(\frac{2D_p^2 \varepsilon}{\mu_p e C}\right)^2. \tag{A5}$$

$$C_1 = -\frac{ep(0)}{\varepsilon} + \frac{\mu_p E^2(0)}{2D_p}. \tag{A6}$$

Let us pick from (A4) a solution that varies monotonically. Hence taking $C_3 = 0$ the equation for the field in the dark we choose takes the form

$$E(x) = \frac{\lambda^{1/3} eC}{D_p \varepsilon}\frac{(\mathrm{Ai})_y}{\mathrm{Ai}(y)}. \tag{A7}$$

This field is not arbitrary since it has first to satisfy condition (A3); it has also to be internally consistent since the variable y depends on $p(0)$ and $E(0)$.

Given (A7) the hole density $p(x)$ is given with (A2) by

$$p(x) = \left(\frac{2\varepsilon}{\mu_p D_p e}\right)^{1/3} C^{2/3}\left[\left(\frac{(\mathrm{Ai})_y}{\mathrm{Ai}}\right)^2 - y\right]. \tag{A8}$$

The condition (A3) may be rewritten with the help of (A7) in the form

$$V = -\frac{2D_p}{\mu_p}\ln\left(\frac{\mathrm{Ai}(y_L)}{\mathrm{Ai}(y_0)}\right) \tag{A9}$$

where y_L and y_0 are the values of y corresponding to $x = L$ and $x = 0$ respectively.

It turns out that in order to determine $E(x)$ and $p(x)$ completely one has to find the values of the unknowns $p(0)$, $E(0)$, C_1 and C. These constants are not independent of each other.

By analysing the relations existing among these, it appears that $E(0)$ may be chosen arbitrarily.

Hence choosing a value for $E(0)$ it is possible to calculate from (A9) the value of $p(0)$ for a given applied potential V and therefore C_1 is obtained from (A6) whereas C is determined from

$$C = -(\mu_p/L)\int_0^L pE\,dx + (D_p/L)[p(L) - p(0)] \tag{A10}$$

which is nothing but the quantity $-J/e$; hence the dark photocurrent is determined.

References

[1] Crine J P, Dorlanne O, Sapieha S and Yelon A 1979 *Annual Report IEEE Conf. on Electrical Insulation and Dielectric Phenomena* p 123
[2] Anderson R A and Kurtz S R, private communication; see also Sawa G, Lee D C and Ieda M 1977 *Japan. J. Appl. Phys.* **16** 359
[3] Crine J P and Yelon A 1980 *J. Appl. Phys.* **51** 2106
[4] Chance R R and Braun C L 1976 *J. Chem. Phys.* **64** 3573
[5] Staebler D L and Wronski C R 1980 *J. Appl. Phys.* **51** 3262
[6] Street R A 1980 *Solid State Commun.* **34** 157
[7] Taylor G W and Simmons J G 1972 *J. Non-Cryst. Solids* **8** 940
[8] Snow E H, Grove A S and Fitzgerald D J 1967 *Proc. IEEE* **55** 1168
[9] Taylor D M 1979 *Radiat. Phys. Chem.* **13** 209
[10] Churchill J N, Holmstrom F E and Collins T W 1979 *J. Appl. Phys.* **50** 3994
[11] Donovan K J and Wilson E G 1981 *Phil. Mag.* B **44** 9
[12] Lampert M A and Mark P 1970 *Current Injection in Solids* (New York: Academic)
[13] Tannous C and Yelon A 1988 *J. Appl. Phys.* **63** 224
[14] Crank J 1984 *Free and Moving Boundary Problems* (Oxford: OUP) p 181
[15] Gear C W 1971 *Numerical Initial-Value Problems in Ordinary Differential Equations* (Englewood Cliffs, NJ: Prentice-Hall)
[16] Bellman R and Wing G 1975 *An Introduction to Invariant Embedding* (New York: Wiley)
[17] Sze S M 1981 *Physics of Semiconductor Devices* 2nd edn (New York: Wiley)
[18] Yano O and Wada Y 1971 *J. Polym. Sci.* A-2 **9** 669
[19] Stutzmann M, Jackson W B and Tsai C C 1985 *Phys. Rev.* B **32** 23